Mathematical Biology

Anti-phase solutions in relaxation oscillators coupled through excitatory interactions

Nancy Kopell[1,*], **David Somers**[2,3,**]

[1] Department of Mathematics, Boston University, 111 Cummington Street, Boston, MA 02215, USA
[2] Department of Cognitive and Neural Systems, Boston University, 111 Cummington Street, Boston, MA 02215, USA
[3] Department of Brain and Cognitive Sciences, Massachusetts Institute of Technology, 45 Carleton Street, E25-618, Cambridge, MA 02139, USA

Received 21 June 1993; received in revised form 11 April 1994

Abstract. Relaxation oscillators interacting via models of excitatory chemical synapses with sharp thresholds can have stable anti-phase as well as in-phase solutions. The mechanism for anti-phase demonstrated in this paper relies on the fact that, in a large class of neural models, excitatory input slows down the receiving oscillator over a portion of its trajectory. We analyze the effect of this "virtual delay" in an abstract model, and then show that the hypotheses of that model hold for widely used descriptions of bursting neurons.

Key words: Neural oscillator – Pulse coupling – Bistability – Synaptic coupling – Van der Pol oscillator

1 Introduction

Neural oscillators are often described by equations with more than one time scale [4, 19, 24, 34]. Such oscillators can be voltage-gated conductance equations qualitatively similar to the Hodgkin–Huxley equations [11], or ensemble equations describing firing rates of excitatory and inhibitory neurons. In both cases, widely used models of interactions between cells are nonlinear, saturating at high and low values of the input. The input can be either excitatory or inhibitory. We show in this paper that even with excitatory interactions alone, a pair of such oscillators can have stable anti-phase solutions as well as stable in-phase solutions. The mechanism for approach to locking for the anti-phase model is very different from that of the approach to synchronous locking, and is also much slower.

* Supported in part by NSF (DMS-8901913), NIMH-47150
** Supported in part by NASA (NGT-50497) and the McDonnell-Pew Foundation

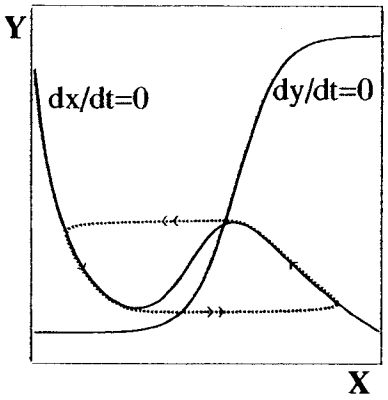

Fig. 1. Nullclines and phase plane trajectory for a single relaxation oscillator (Morris–Lecar). When the relaxation parameter, ε, is small the trajectory slowly traverses the outer branches of the cubic-shaped nullcline toward the local extremum of each branch. When an extremum is reached, the trajectory jumps rapidly to the other branch

We shall be interested in equations of the form

$$\varepsilon x' = F(x, y) \tag{1}$$

$$y' = G(x, y)\,, \tag{2}$$

having a stable limit cycle and $\varepsilon \ll 1$. The nullcline $F(x, y) = 0$ should be cubic shaped as in the van der Pol oscillator and other equations associated with descriptions of neurons and assemblages of neurons. (See Fig 1.) When ε is very small, the resulting limit cycle then has four pieces, two of which are traversed much faster than the other two. The two slow pieces stay close to the outer branches of the cubic $F(x, y) = 0$. (See Fig 1.)

We now consider a coupled pair of oscillators. The coupling we consider changes (1) to

$$\varepsilon x' = F(x, y, I[\hat{x}])\,, \tag{3}$$

where $\hat{x}$ denotes the x-variable of the other oscillator, and $I[\hat{x}]$ is the coupling signal. We assume that $I[\hat{x}]$ is a saturating sigmoidal function having a ramp that lies entirely in the middle branch of each of the cubic curves $F(x, y, I) = 0$ for all values of I in the range of the function $I[\hat{x}]$. (See Fig 2a, b.) In particular, we assume that I is a constant on each of the two outer branches, $I = I^+$ or $I = I^-$, depending on whether $\hat{x}$ lies on the right or left branch. In the relaxation limit, this is equivalent to assuming that I is a step function, with threshold that lies in the middle branch of each of the relevant cubics. In [28], we referred to such coupling as "Heaviside Coupling." We also assume about the coupling signal that if $F(x, y, I) = 0$ is solved for $y = f(x, I)$, then $\partial f/\partial I > 0$. Thus, increasing I lifts the graph of y vs. x, possibly with a change of shape. (See Fig 2b). Such an assumption corresponds to excitatory input for neural oscillators, either in single neuron conductance based models such as Hodgkin–Huxley [11] and Morris–Lecar [19] or ensemble descriptions such as Ellias–Grossberg [4] or Wilson–Cowan [34].

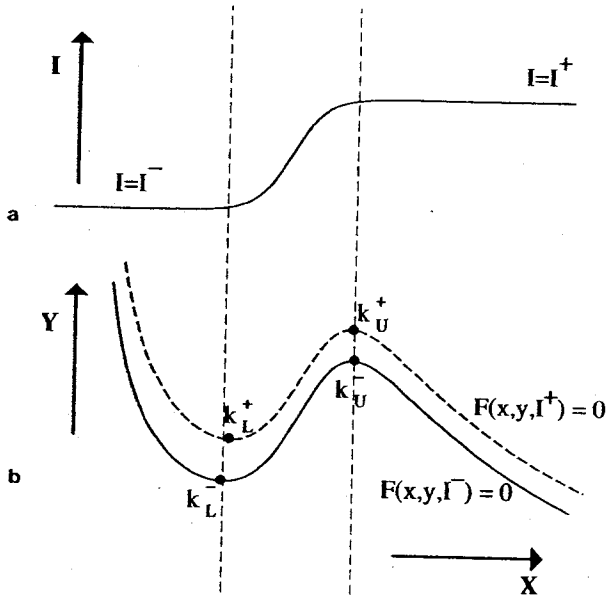

Fig. 2a, b. Heaviside Coupling. **a** shows a sigmoidal coupling function, $I(x)$, for which the non-constant ranges of the function lie in the middle branch of the cubic nullcline. Since the phase-plane trajectory hugs the outer branches and rapidly jumps between the branches, the coupling function assumes one of two constant values, I^- or I^+, determined by the branch on which the input oscillator lies. I^- or I^+ define different cubic nullclines with the I^+ nullcline shifted upward, possibly with a change of shape as shown in **b**. The trajectory of a coupled pair of identical oscillators can be described by these two cubics and the rapid transitions between them. The local extremum or "knees", k_L^-, k_L^+, k_U^-, and k_U^+, are important transition points

In a previous paper [28] we showed that under the above assumptions there is a stable in-phase solution to a pair of coupled oscillators. That paper focuses on the determinants of the rate at which the in-phase solution is approached, and describes a mechanism of approach to synchrony that has properties quite different from those associated with equations coupled through phase differences. It also discusses the consequences of this mechanism for the rate of approach to synchrony in a long array of oscillators.

In the current paper, we are concerned with *anti-phase* solutions to (2)–(3) describing a pair of neural-like oscillators still interacting via *excitatory* coupling. As we will show, the existence of such solutions for these equations requires further hypotheses; the essential hypothesis is one on the "duty cycle" of the oscillators, i.e., that the time spent along the two branches are significantly unequal. The mechanism of approach to phase-locking in the anti-phase configuration is more subtle than that of approach to synchrony. It uses the existence of regions of initial conditions in which one oscillator stays on the longer (in time) branch during the entire excursion of the other on the

shorter branch. During that time, the first oscillator is displaced from the orbit it would have had, and travels along the displaced branch at an altered speed. This leads to a "virtual delay" for the first oscillator due to the excursion of the second (even though the coupling is excitatory, and leads to advances in other regions of initial conditions). If this delay function satisfies a convexity condition reminiscent of pulse coupling models of Peskin [22] and Mirollo and Strogatz [18], we show that there is a stable anti-phase solution. Furthermore, we show that this mechanism holds for large classes of neural-like oscillators. We demonstrate that in some parameter ranges of those classes, both the in-phase and anti-phase solutions are stable.

It is well-known that a pair of oscillators weakly or moderately coupled can cometimes have both in-phase and anti-phase trajectories as stable solutions [10, 23, 26]. Provided that the coupling is not too strong, the behavior is approximated by the phase models in which the coupling can be described in terms of a periodic function H of the phase difference between the oscillators. If the function $[H(\phi) + H(-\phi)]/2 \equiv f(\phi)$ has zeros at $\phi = 0$ and $\phi = \pi$, and $f'(0) > 0$, $f'(\pi) > 0$, both in-phase and anti-phase solutions are stable [6]. Such phase models are not appropriate for relaxation oscillators coupled at moderate to strong strengths, since the movement in phase space is not then restricted to a neighborhood of the limit cycle.

In-phase and anti-phase solutions have also been investigated for relaxation oscillators interacting through linear coupling [1, 21, 30], and bistability has been found. The nonlinear coupling used in this paper, appropriate for the description of interacting neurons, allows the oscillators to be treated as if they were partially uncoupled, reducing the dimensions of the spaces in which the calculations must be made. In particular, unlike [1, 21, 30], our proof of existence and stability of the anti-phase solution reduces to the proof that a certain map in one dimension has a stable critical point. Another paper that reports stable anti-phase solutions with linear coupling (diffusion in one variable) is [27]. In that case, the coupling is not strong and the mechanism appears to be closely related to that of phase models. The work here and in [28] also contrasts with [33], who report bistability in oscillators coupled via *inhibition*. In [33], the in-phase solution depends critically on slowly changing synaptic inputs, while we use interactions that do not introduce another slow variable. Other related literature on a pair of coupled oscillators includes [5, 13, 14, 20, 32] (For other related references see [3, 7, 12].)

The existence of simultaneous in-phase and anti-phase solutions for (2), (3) allows new behavior for an array of oscillators, such as a long chain (or circular array) pairwise coupled as above. The new behavior is "fractured synchrony", in which domains of oscillators are in synchrony, but are anti-phase with neighbor domains. In [15] we shall explain why such behavior can be achieved by oscillators of the form (2)–(3), but not generally by oscillators coupled through phase differences, even those which pairwise have stable in-phase and anti-phase solutions.

2 A pulse coupling model of anti-phase behavior

We shall first analyze the behavior of (2), (3) in the singular limit, and reduce the existence of the anti-phase solution to that of a fixed point of a 1-D map. The structurally stable behavior of that 1-D map is then used to achieve the anti-phase result for $\varepsilon > 0$.

The key feature of Heaviside coupling [28] is that the coupling term in the equation for oscillator 1 depends on whether oscillator 2 is at a value above or below the threshold for the function $I[\hat{x}]$. With that threshold chosen to be on the middle branch of each of the cubics $F(x, y, I) = 0$, the coupling gives information only about which of the two outer branches of a cubic oscillator 2 is on. Thus, oscillator 1 is governed by (2) and one of the two equations

$$\varepsilon x' = F(x, y, I^{\pm}) . \tag{4}$$

In the limit of ε small, this implies that the solution to the coupled system is made up of pieces of the outer branches of the cubics $F(x, y, I^{\pm}) = 0$ plus the rapid transitions between these pieces. These cubics are sketched in Fig 2b. Of particular importance will be the local minimum of each of these curves, labeled k_L^- and k_L^+ and the local maximum of each, labeled k_U^- and k_U^+.

Jumps between pieces of the branches occur when one of the oscillators reaches its branch minimum or maximum. The jump changes the coupling input to the other oscillator, which must then travel along a piece of the other cubic. Depending on initial conditions, this may or may not induce a jump of the second oscillator to a branch at the other side of the threshold. (See Fig 3a.) We denote by $j^+(p)$ the image of a point p after a jump to the I^+ cubic, and similarly denote by $j^-(p)$ jumps to the I^- cubic.

The singular trajectory corresponding to in-phase behavior is sketched in Fig. 3b. Note that since $x = \hat{x}$ for the synchronous solution, the coupling function has input I^+ when x is on a right branch and I^- when x is on a left branch. Thus the trajectory lies on the upper cubic on the right and the lower cubic on the left. The anti-phase solution we shall construct will have a more complicated singular trajectory, using the right branch of the lower cubic and parts of the left branches of both cubics.

The in-phase solution occurs very stably under very robust circumstances described in Somers and Kopell [28]. To get the anti-phase solution in the relaxation regime, we require similar hypotheses plus an additional restriction. This restriction is that the relative amount of time needed to traverse right and left branches of the cubics be unequal, so that there is some range of initial conditions for which only one oscillator at a time traverses one of the branches. For definiteness, we assume that the right hand branch is the shorter one. The following condition then spells out the restriction.

Condition D. The time τ to traverse the right branch of $F(x, y, I^-) = 0$ from the rightward jump point $j^-(k_L^-)$ to the branch maximum point at k_U^- is less than the time $\hat{\tau}$ on the left branch of $F(x, y, I^+) = 0$ from the leftward jump point $j^+(k_U^-)$ to the branch minimum at k_L^+. (See Fig 3c.)

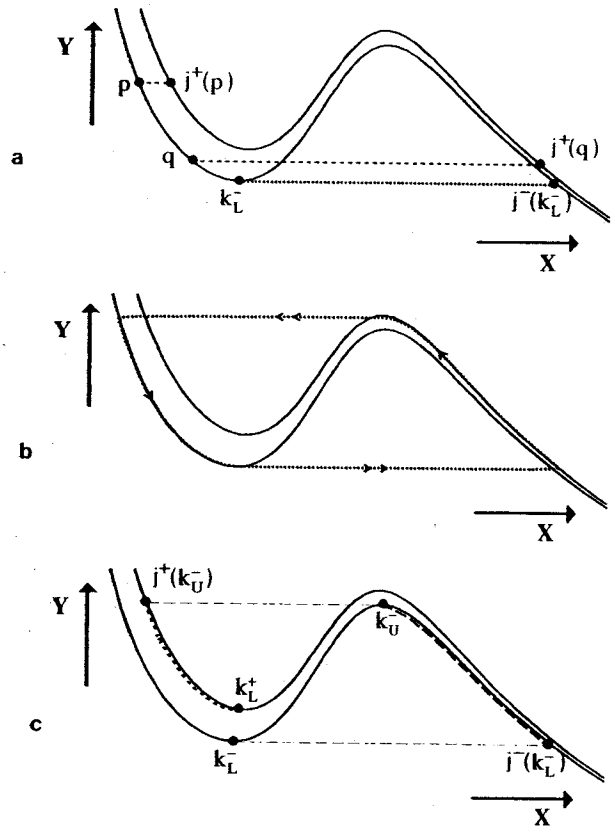

Fig. 3. a demonstrates the effects of Heaviside coupling on a trailing oscillator (*dashed line*) when the leading oscillator (*dotted line*) reaches its local extremum, k_L^-. The lead oscillator jumps to the right branch of the I^- cubic, thus increasing the coupling to the trailing oscillator and causing it to jump to the I^+ cubic. If the trailing oscillator lies below the knee of the raised nullcline, as for point q, the trailing oscillator will jump immediately to right branch. However, if the oscillator trails by a greater amount, as does point p, the jump is to the left branch of I^+. **b**: The limiting synchronous solution is composed of the left branch of the I^- and the right branch of the I^+ cubics. c illustrates Condition D. The anti-phase solution requires that the time required to traverse the right branch of the I^- cubic, from the point $j^-(k_L^-)$ reached on a jump from k_L^- to the branch maximum point k_U^-, be less than the time required to traverse the left branch of the I^+ cubic, from the point $j^+(k_U^-)$ reached on a jump from k_U^- to the branch minimum point k_L^+

Remark 2.1. Condition D is related, but not equivalent, to a condition on the "duty cycle" (or ratio of time on the right hand branch τ to time on the both branches) of the *uncoupled* oscillators. In general, Condition D is expected to hold whenever the duty cycle of the uncoupled oscillator is significantly less than 1/2 and the coupling is not too strong. Increasing the coupling strength (i.e., increasing the difference between I^+ and I^-) increases the difference between the two cubics. This makes the leftward jump point $j^+(k_U^-)$ closer to

the minimum k_L^+ of $F(x, y, I^+)$; therefore, it can decrease the time $\hat{\tau}$ on the left hand (longer) branch of the $I = I^+$ cubic, and thus make the times in Condition D more equal. For large enough coupling, the leftward jump point $j^+(k_U^-)$ is equal to k_L^+, and so $\hat{\tau} = 0$; it follows that at some smaller coupling strength, Condition D ceases to hold.

We shall now show that, in the presence of Condition D, we can analyze the trajectories for some class of initial conditions in terms of "fictive pulses". The input from the Heaviside coupling we are employing determines the cubic along which a given oscillator is constrained to move. Furthermore, the rate of change of y along the left branch (or right branch) is different for the two cubics. Thus the excursion of one oscillator to the right hand branch affects the rate of speed of the vertical motion of the other in a manner that depends on the position of the second oscillator. We shall first analyze these changes in particularly well-suited coordinates. We give hypotheses in these coordinates that are sufficient to produce the anti-phase behavior. Later we shall show that these hypotheses actually hold for a large collection of neural-like oscillators.

2.1 The pulse model

We consider the left hand branch of $F(x, y, I^-) = 0$, and parameterize it so that the motion along it is uniform in time. That is, we replace y by $z(y)$ such that dz/dt is constant and positive. Thus, z is a measure of phase. We may assume that $z = 0$ corresponds to the position on that branch just after the leftward jump from k_U^-, and $z = 1$ to the position just before the rightward jump from k_L^-. (See Fig 4a.) Furthermore, by rescaling, we may assume that $dz/dt \equiv 1$. Under that rescaling, let $\bar{\tau}$ be the time corresponding to time τ in the old time scale.

We are interested in a subset of trajectories for which oscillator 1 starts at k_L^- and oscillator 2 starts with a value of z in $[0, 1]$. Oscillator 1 jumps immediately to the right hand branch of $F(x, y, I^-) = 0$, causing oscillator 2 to jump to the left hand branch of $F(x, y, I^+) = 0$. We restrict ourselves to the subinterval J of $[0, 1]$ consisting of those z small enough that oscillator 2 does not reach k_L^+ in the time $\bar{\tau}$ it takes oscillator 1 to reach k_U^-. By Condition D, there are such points.

After time $\bar{\tau}$, oscillator 1 jumps back to the left hand branch of $F(x, y, I^-) = 0$, causing oscillator 2 to return to this branch. Thus, for each z in J, we have a map $z \mapsto E(z)$, the new position of oscillator 2 when oscillator 1 returns to the left branch $\bar{\tau}$ units later (see Fig 4b). Since oscillator 2 does not change its direction during the excursion of oscillator 1 to the right hand branch, we have $E(z) > z$; it follows from the uniqueness theorem of ordinary differential equations that E is monotone increasing and hence $E'(z) \geqq 0$. The domain of E is J. Note that $J \equiv [0, \bar{z}]$, where $\bar{z}$ is defined as follows: Let p^+ be the point on the left hand branch of the $I = I^+$ cubic such that the (scaled) time

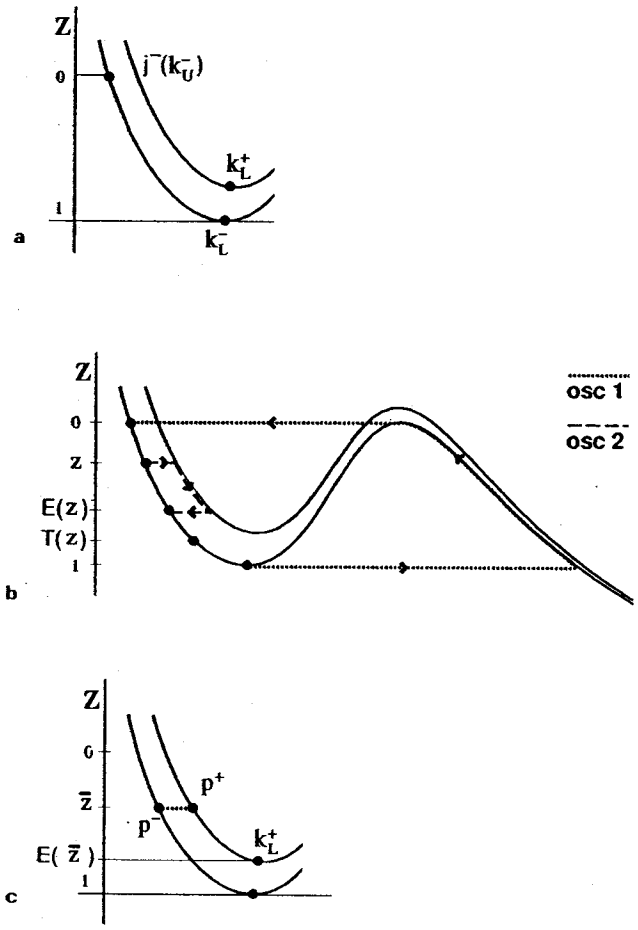

Fig. 4a–c. Pulse coupling model. **a**: The left branch of the I^- cubic is parameterized by z, such that 0 represents the point $j^-(k_U^-)$ reached on a jump from k_U^-, 1 represents k_L^-, and time moves uniformly for z. **b**: Provided that Condition D is met, initial conditions exist for which the leading oscillator may traverse the right branch and return to the left, while the trailing oscillator remains on the left branches. For the duration of the excursion the trailing oscillator is "pulsed" to the left branch of the I^+ cubic. For z the value of the trailing oscillator at the start of an excursion, the map $E(z)$ gives the position at the end of the excursion. The map $T(z)$ describes where the trailing oscillator would have gone in the same amount of time had the excursion not occurred. **c**: $\bar{z}$ is the upper bound of the domain of the map E. p^- and p^+ are the corresponding points on the I^- and I^+ cubics (see text). For $z > \bar{z}$, the trailing oscillator jumps to the right branch before the excursion of the lead oscillator is completed

from p^+ to k_L^+ is $\bar{\tau}$. (Such a point is guaranteed to exist because of Condition D.) Let p^- be the point on the $I = I^-$ cubic with the same y value, and $\bar{z}$ be the z-coordinate value of this point (see Fig 4c).

We also have the map $z \mapsto T(z) \equiv z + \bar{\tau}$, the new position of z after the same amount of time in the absence of excitation. For the class of oscillators

we are concerned with, including the Morris–Lecar oscillator and the Ellias Grossberg network oscillator, it will be shown below that $E(z) < T(z)$. Hence we refer to the map $\Delta(z) \equiv T(z) - E(z)$ as the "virtual delay map"; Δ measure the disparity between where oscillator 2 actually is at the end of the excitatio vs. where it would have been in the absence of excitation. We now giv conditions on $E(z)$, or equivalently $\Delta(z)$, that guarantee the existence o a locally unique stable anti-phase solution.

Proposition 2.1. *Suppose that Condition D holds and*
(i) $E(0) > 0$.
(ii) *E is monotone increasing with $0 \leqq E'(z) < 1$ (the last inequality is equivalent to $\Delta'(z) > 0$).*
(iii) $E(\bar{z}) > 1 - \bar{z}$.
Then there is a stable anti-phase solution. This solution corresponds to a stable fixed point of the map $M(z) \equiv 1 - E(z)$. Its domain of stability includes J if $E(0) \geqq 1 - \bar{z}$ and a subset of J otherwise.

Proof of Proposition 2.1. To see that a fixed point of the map $M(z)$ corresponds to an anti-phase solution, we note that M is the map whose input is the initial position z of oscillator 2 when oscillator 1 is at $z = 1$, and whose output is the position of oscillator 1 when oscillator 2 reaches $z = 1$. (If oscillator 1 is initially at $z = 1$ when oscillator 2 is at $0 < z < \bar{z}$, then $\bar{\tau}$ units later, oscillator 1 is at $z = 0$ (the end of its excursion) and oscillator 2 is at $E(z)$. See Fig 4b. By hypotheses i) and ii) $E(z) > 0$, so oscillator 2 now leads oscillator 1. It takes $1 - E(z)$ units more for oscillator 2 to reach $z = 1$; at that time, oscillator 1 is at position $1 - E(z)$.) It follows from this characterization that a fixed point, z_f, of M lies on a periodic anti-phase solution with period (in scaled time) twice the time $(\bar{\tau} + 1 - E(z_f))$ it takes from z_f to the jump point $z = 1$.

To show that $M(z)$ has a stable fixed point, we show that there is a subset of $[0, \bar{z}]$ that maps into itself, and that $|M'(z)| < 1$. If $E(0) \geqq 1 - \bar{z}$, then by the monotonicity of E we have $E([0, \bar{z}]) \subset [1 - \bar{z}, 1]$, so M maps $[0, \bar{z}]$ into itself. From hypothesis ii) and the definition of M, $-1 < M'(z) \leqq 0$. (Note that since E is order preserving on z, M is order reversing.) If $E(0) \leqq 1 - \bar{z}$, then $M(0) = 1 - E(0) \geqq \bar{z}$. Also by hypothesis iii) $M(\bar{z}) = 1 - E(\bar{z}) < \bar{z}$. Using the monotonicity of E from hypothesis ii) there is a unique point $0 \leqslant \underline{z} < \bar{z}$ such that $M(\underline{z}) = \bar{z}$. M is order reversing so points below $\underline{z}$ map to points above $\bar{z}$; Since $|M'(z)| < 1$, it follows that the interval $[\underline{z}, \bar{z}]$ maps strictly into itself with $M(\bar{z}) > \underline{z}$. Thus, we are done. □

Remarks

2.2. In their pulse coupling model, Mirollo and Strogatz [18] required the phase speedup caused by a pulse to increase as threshold is approached. That condition is equivalent to requiring that the phase response function be convex. Under that condition, a positive pulse leads to a stable in-phase solution. Our condition $\Delta'(z) > 0$ requires that the size of the virtual delay (the

existence of which will be demonstrated for our examples in Sects. 2.2 and 3 increase as threshold is approached; thus it resembles a negative-pulse convexity condition. However, the oscillators treated here differ from the "integrate-and-fire" model in that the excursion time is non-zero and thus the trailing oscillator not only is pulsed backward but also advances during the excursion.

2.3. The convexity condition $\Delta'(z) > 0$ implies that the fixed point is locally unique. In its absence, it may be possible to get a whole interval of fixed points, corresponding to a continuum of anti-phase solutions with different frequencies. Such a family of solutions appear to be in a related model of Krinskii et al. [16], which uses a condition like our Condition D. The computer simulations in that paper, of which their model is a caricature, show the characteristic indentation of Fig 4b, though the caricature assumes that the trajectories stay on the branches of the cubic, thus ignoring the effects of virtual delay.

2.4. Hypothesis iii) is stronger than Condition D. The latter requires that there is an interval $J = [0, \bar{z}]$ of initial conditions for oscillator 2 such that oscillator 2 remains on the left branch during the excursion of oscillator 1. By contrast, hypothesis iii) requires the stronger condition that for some subset of $[0, \bar{z}]$ oscillator 1 *also* stays on the left branch during the subsequent excursion of oscillator 2. To see this we note that hypothesis iii) can be rewritten as $M(\bar{z}) \equiv 1 - E(\bar{z}) < \bar{z}$. If this holds, then there is a subinterval of z near $\bar{z}$ for which $M(z) < \bar{z}$. Since $M(z)$ is the position of oscilator 1 when oscillator 2 reaches its jump point $z = 1$, by definition of $\bar{z}$, $M(z) < \bar{z}$ means that oscillator 1 stays on the left branch during the excursion of oscillator 2. Hypothesis iii) can easily be verified in computer simulations by observing the jumps in the time course of the fast variables, x_i, for (less than) the first two cycles.

2.5. The rate of attraction of the anti-phase solution depends on $\Delta'(z) \equiv T'(z) - E'(z) \equiv 1 - E'(z)$ over the domain of attraction. Below in Proposition 2.2 and in Sect. 3 we show that the delay conditions $z < E(z) < T(z) \equiv z + \bar{\tau}$ are satisfied for broad classes of neural oscillators including our specific examples. Provided that $z < E(z) < T(z)$, it follows that as $\bar{\tau}$ decreases so does $|E'(z) - 1|$. Thus the rate of attraction of the anti-phase state also decreases. However, the domain of attraction of this state does not necessarily shrink with decreasing $\bar{\tau}$. As stated in Proposition 2.1, the size of the domain is governed by $E(0)$, and this domain can remain $O(1)$ even if $\bar{\tau} \mapsto 0$.

The approach to the in-phase mode, as described in [28], is much faster than the approach to the anti-phase mode. As shown in [28], the geometric rate of approach to the in-phase solution depends on the "compression" in time differences that occurs across jumps; this can be as much as a factor of 10 in some examples. See Remark 2.9 for more details about compression.

2.6. Measured in scaled time, the period of the uncoupled oscillator is $1 + \bar{\tau}$, where 1 and $\bar{\tau}$ are the times on the left hand branch and right hand branch respectively. Provided that $E(z) < T(z)$, the anti-phase solution has a longer period because the time on the left branch is increased by $\Delta(z_f) > 0$, where z_f is

the fixed point. The in-phase solution may have either a longer or shorter period than the uncoupled oscillator, but without further hypotheses on the relative speeds along the two right branches we cannot say which.

2.7. The above analysis describes the case in which the time to traverse the excited branch of the cubic is shorter than that for the unexcited one. In the opposite case, for nerve-like equations, traversal of the short branch still creates virtual *delays* on the longer branch. The essential reason for the delay is that the excursion of one oscillator constrains the other oscillator to move onto a branch of a cubic that is closer to the y-nullcline, along which $|y'|$ is smaller.

Proposition 2.1 deals with the singular limit $\varepsilon \mapsto 0$. It turns out the same hypotheses suffice to conclude the existence of a stable antiphase solution for $0 < \varepsilon \ll 1$. The proof of this statement uses deeper ideas from dynamical systems and will be done in the appendix as Proposition A.1.

2.2 Physical models and the pulse description

The abstract conditions shown above (and in the appendix) to be sufficient for the stable existence of anti-phase solutions are satisfied for large classes of neural oscillators. In order to show this, we now translate the conditions of Proposition 2.1 to hypotheses on the functions F and G in the original variables. We also give conditions on F and G to show that $E(z) < T(z)$. This will be used in Sect. 3 to show that, for the class of examples we consider, excitatory coupling creates delays. In Sect. 3, we whow how these conditions apply to a pair of specific classes of equations.

Let $x = h^+(y)$ be the solution to $F(x, y, I^+) = 0$ along the left hand branch of the latter, and $x = h^-(y)$ be the solution to $F(x, y, I^-) = 0$, also along the left hand branch.

Proposition 2.2. *Provided that Condition D holds*
(i) Sufficient conditions for $z < E(z) < T(z)$ *are*

$$G(x, y) < 0 \text{ along } F(x, y, I^+) = 0 ,$$

and

$$\frac{\partial}{\partial x}[G(x, y)] > 0 , \tag{5}$$

over the region between the left branches of the two cubics.
(ii) Sufficient conditions for $\Delta'(z) > 0$ *are*

$$\frac{d}{dy}[G(h^-(y), y) - G(h^+(y), y)] > 0 , \tag{6}$$

along the left branches of the two cubics, and

$$\frac{d}{dy} G(h^-(y), y) < 0 , \tag{7}$$

along the left branch.

Remark 2.8. Proposition 2.2 does not give conditions for hypothesis iii) of Proposition 2.1. Unlike hypothesis ii) which gives conditions on the oscillator equations, hypothesis iii) applies primarily to the existence of initial conditions with certain properties. As discussed in Remark 2.4, it is easy to directly verify hypothesis iii) for a system of equations. This hypothesis does hold for the specific examples to be discussed in Sect. 3. As mentioned before the statement of Proposition 2.1, the hypotheses of monotonicity and $0 \leqq E'(z)$ follow from general properties of differential equations.

Proof of Proposition 2.2. (i) Since $G(x, y) < 0$ along the left branches, (2) implies that $y' < 0$. Since z increases as y decreases, this implies that $z < E(z)$ (and in particular, $E(0) > 0$). The inequality $E(z) < T(z)$ says that the distance traversed by one oscillator during the excursion of the other on the right hand branch is less than the distance that would have been traveled in the absence of the excursion. This holds provided the rate of (downward) movement on the $I = I^+$ cubic is smaller than the rate at the same value of y on the $I = I^-$cubic, or equivalently (using $G(x, y) < 0$), $G(h^+(y), y) - G(h^-(y), y) > 0$. Since $h^+(y) > h^-(y)$, the latter condition holds provided that (5) holds.

(ii) In unscaled time, starting from a point y on either the I^+ or I^- cubic, a trajectory moves to $y^\pm \equiv \int_0^\tau G(h^\pm(\bar{y}), \bar{y})\, dt$ in τ time units, where $\bar{y} = \bar{y}(t; y)$ satisfies $\bar{y}(0) = y$. We denote these functions by $y^\pm = Y^\pm(y)$. Let $z = Z(y)$ be the transformation between the y coordinates and the z coordinates. In terms of z, the functions $Y^\pm(y)$ are $Z(Y^\pm(Z^{-1}(z)))$. $T(z) - z$ is the distance covered on the I^- cubic in time τ, while $E(z) - z$ is the distance covered in the same time on the I^+ cubic. Thus

$$\Delta(z) \equiv T(z) - E(z) = [Z(Y^-(Z^{-1}(z))) - z] - [Z(Y^+(Z^{-1}(z))) - z]\,.$$

Therefore,

$$\begin{aligned}
\Delta'(z) &= [Z'(y^-)][(Y^-)'(Z^{-1}(z))][(Z^{-1})'(z)] \\
&\quad - [Z'(y^+)][(Y^+)'(Z^{-1}(z))][(Z^{-1})'(z)] \\
&= [Z'(y^-)][(Y^-)'(Z^{-1}(z))][(Z^{-1})'(z)] \\
&\quad - [Z'(y^-)][(Y^+)'(Z^{-1}(z))][(Z^{-1})'(z)] \\
&\quad + [Z'(y^-)][(Y^+)'(Z^{-1}(z))][Z^{-1})'(z)] \\
&\quad - [Z'(y^+)][(Y^+)'(Z^{-1}(z))][(Z^{-1})'(z)]\,.
\end{aligned}$$

This simplifies to

$$\begin{aligned}
\Delta'(z) &= [Z'(y^-)][(Z^{-1})'(z)][(Y^-)'(Z^{-1}(z)) - (Y^+)'(Z^{-1}(z))] \\
&\quad + [Z'(y^-) - Z'(y^+)][(Y^+)'(Z^{-1}(z))][(Z^{-1})'(z)]\,. \qquad (8)
\end{aligned}$$

$\Delta'(z) > 0$ is satisfied if both terms of (8) are positive. Since Z is direction reversing, $Z'(y^{\pm}) < 0$ and $(Z^{-1})'(z) < 0$. Since $Z^{-1}(z) = y$,

$$[(Y^-)'(Z^{-1}(z)) - (Y^+)'(Z^{-1}(z))] = \frac{d}{dy}[Y^-(y) - Y^+(y)]$$

$$= \frac{\partial}{\partial y}\int_0^\tau G(h^-(\bar{y}), \bar{y}) - G(h^+(\bar{y}), \bar{y})\,dt$$

$$= \int_0^\tau \frac{d}{dy}[G(h^-(\bar{y}), \bar{y}) - G(h^+(\bar{y}), \bar{y})]\,dt\,.$$

Thus the hypothesis that $\frac{d}{dy}[G(h^-(\bar{y}), \bar{y}) - G(h^+(\bar{y}), \bar{y})] > 0$ is sufficient to guarantee that the first term of the right hand side of (8) is positive.

From the definition it is clear that $(Y^+)'(y) > 0$. Therefore, it is sufficient to show that $Z'(y^-) - Z'(y^+) < 0$ in order to show that the second term of the right hand side of (8) is positive. Since $y^- < y^+$, it is sufficient to show that $Z''(y) > 0$. We have a formula for $Z(y)$; up to a positive constant factor, $Z(y)$ is the time it takes to go from $j^-(k_U^-)$ to y along the left branch of $I = I^-$. Let $cZ(y)$, $c > 0$ be that time. Then

$$y - y_0 = \int_0^{cZ(y)} G(h^-(\bar{y}(t)), \bar{y}(t))\,dt\,,$$

where $y_0 = h^-(\bar{y}(0))$ = the y value at $j^-(k_U^-)$. Differentiating both sides with respect to y yields,

$$1 = cZ'(y)G(h^-(y), y)\,.$$

Differentiating again yields

$$0 = Z''(y)G(h^-(y), y) + Z'(y)\frac{d}{dy}G(h^-(y), y)\,.$$

Since $Z'(y) < 0$ and $G(h^-(y), y) < 0$, it follows that $\frac{d}{dy}G(h^-(y), y) < 0$ is sufficient to guarantee that $Z''(y) > 0$, and thus that the second term of the right hand side of (8) is positive. □

Remark 2.9. Condition (7) is closely related to the central condition needed for stability of the in-phase solution. That requirement, called "Condition C" in [28], concerns initial conditions for which one oscillator is at a jump point k_L^- (or k_U^+) and the other at a point, q, is sufficiently close (on the same branch) that the change in nullcline due to the change in coupling will cause it to jump immediately thereafter. (See Fig 3a.) The condition is that the amount of time needed to go from q to k_L^- is greater than the time between their images $j^+(k_L^-)$ and $j^+(q)$ on the other branch. As shown in Somers and Kopell [28], the difference in time creates a compression in phase difference across the jump, which in turn suffices to produce stability for the synchronous solution in the singular limit.

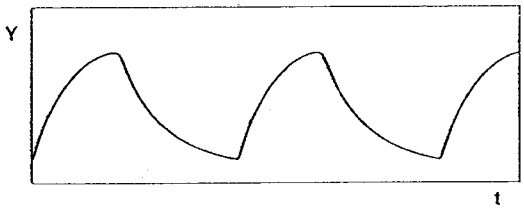

Fig. 5. Slow variable time course for the Morris–Lecar oscillator. The time required to traverse a y interval increases as threshold (a "knee") is approached. This "scalloped" shape of the time course ($y' \cdot y'' < 0$) satisfies both Condition C for the in-phase solution and condition (7) for anti-phase

Condition C holds whenever the time course of $y(t)$ in the synchronized solution has a "scalloped" shape as in Fig. 5. The ratio of the slopes of y just before to just after a local maximum or minimum is a measure of the compression. (See [28] for more details.) Since $G(h^-(y), y)$ is the rate of y along the left hand branch of the I^- cubic, condition (7) holds exactly when the graph of $y(t)$ along this branch is concave up as in the decreasing parts of the graph in Fig. 5.

3 Specific examples

We now introduce the equations for model neural oscillators and show how the theory of Sect. 2 applies to these equations. We also discuss the in-phase and anti-phase solutions to equations for pairs of these oscillators. We shall use two types of models of nerve cells, one a cellular-level description that is a standard simplification of one-compartment Hodgkin–Huxley models; the second in an ensemble description.

The Morris–Lecar system [19] is an example of voltage-gated conductance equations. These equations are used as a simplified description of an action potential, or as the envelope of a burst [25]. The equations for a single oscillator are

$$dx/dt = -g_{Ca} m_\infty(x)(x-1) - g_K y(x - x_k) - g_L(x - x_L) + I_{ext} \tag{9}$$

$$dy/dt = \lambda[y_\infty(x) - y]/\tau_y(x) \tag{10}$$

where

$$m_\infty(x) = 0.5[1 + \tanh\{(x - x_1)/x_2\}],$$

$$y_\infty(x) = 0.5[1 + \tanh\{(x - x_3)/x_4\}],$$

$$\tau_y(x) = 1/\cosh\{(x - x_3)/(2x_5)\}.$$

The nullclines for these equations, and singular limit cycle, are drawn in Fig. 1. The parameter values are $x_1 = -0.01$, $x_2 = 0.15$, $x_3 = 0.1$, $x_4 = 0.145$, $x_5 = 0.29$, $g_{CA} = 1.0$, $g_L = 0.5$, $g_K = 2.0$, $x_L = -0.4$, $x_K = -0.7$, $\lambda = 0.005$. I_{ext} ranged from 0.05 to 0.15 in different trials. For these parameters, the duty

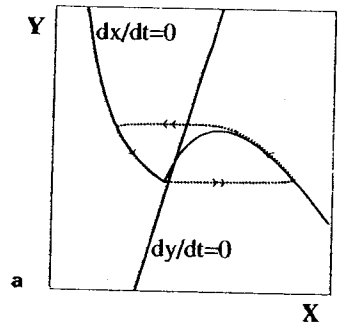

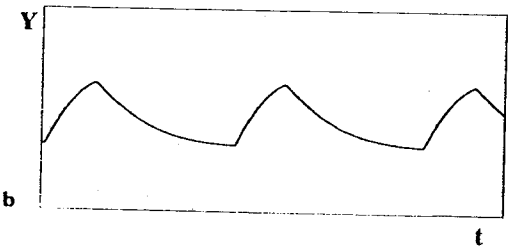

Fig. 6a, b. Ellias–Grossberg oscillator. **a**: nullclines and phase plane trajectory resemble those of Morris–Lecar shown in Fig 1. **b**: Slow variable time course exhibits "scalloped" shape similar to Morris–Lecar (Fig. 5)

cycle is less than one-half. The coupling between a pair of such oscillators is given, as described in Sect. 2, by adding the term

$$-\alpha g_{Ca} m_\infty(\hat{x})(x-1) \tag{11}$$

to (9), where $\hat{x}$ denotes the voltage of the other oscillator and α represents the coupling strength. α was varied between 0.0 and 0.2 in different trials.

The ensemble equations that we use are the Ellias–Grossberg equations [4]. For a single oscillator, these equations are

$$dx/dt = -Ax + (B-x)\{C[x-\Gamma]^+ + I_{ext}\} - Dx[y-\Gamma]^+ \tag{12}$$

$$dy/dt = E(x-y) \tag{13}$$

where $[s]^+ \equiv \max(s, 0)$. The variable x represents the potential of an excitatory cell governed by a nonlinear, shunting equation (Grossberg [8, 9]; Sperling and Sondhi [29]; y represents the potential of an inhibitory cell governed by a linear equation. The parameters for (12)–(13) are $A = 1$, $B = 1$, $C = 20$, $D = 33.3$, $E = 0.02$, $\Gamma = 0.4$. I_{ext} ranged from 1.0 to 2.0 in different trials. The nullclines for (12)–(13) and the oscillation in the singular limit are given in Fig. 6a. Two such systems are coupled by adding

$$\alpha(B-x)[\hat{x}-\Gamma]^+$$

to (12). The coupling strength, α, was varied between 0.0 and 0.2 in different trials.

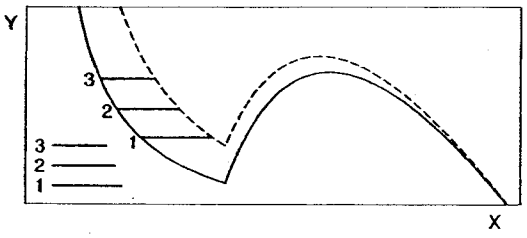

Fig. 7. Sufficient condition (6) for anti-phase solutions in Ellias–Grossberg simplifies to a expression which compares the change in the x-distance between the nullclines as a functic of y. This can be verified by visual inspection; the bars get shorter as y increases

We now discuss conditions (5)–(7) for the above equations. Condition (5) easy to check for both kinds of equations. For the Ellias–Grossberg equation $G(x, y) = c[k(x) - y]$, with $c > 0$ and $k'(x) > 0$. Thus $(\partial/\partial x)G(x, y) > 0$. Fc the Morris–Lecar equations $G(x, y) = m(x)[k(x) - y]$, with $m(x) > 0$, an $k'(x) > 0$. Over the region between the left branches of the two cubic $[k(x) - y] < 0$, and $m'(x) < 0$. Therefore, we again have $(\partial/\partial x)G(x, y) > 0$.

Condition (7) has been shown in Remark 2.9 to be related to the shape c the time course of the slow variable. In Figs. 5 and 6b, we give plots of $y(t)$ fo the Morris–Lecar and Ellias–Grossberg oscillators, respectively, for the syn chronous solution, in which the decreasing portion takes place along th branch in question for condition (7). Note the appropriate concave shape.

Condition (6) is harder in general to verify, but can be done if $G(x, y)$ ha the form $c[k(x) - y]$, provided $c > 0$, $k' > 0$ and $k'' \geqq 0$ as in Ellias–Gros sberg. We now show how to reduce (6) in this case to a simpler system that ca be checked visually. Using the chain rule, condition (6) is

$$c\left[k'(h^-(y))\frac{dh^-(y)}{dy} - k'(h^+(y))\frac{dh^+(y)}{dy}\right] > 0$$

or

$$c\left(\left[k'(h^-(y))\frac{dh^-(y)}{dy} - k'(h^-(y))\frac{dh^+(y)}{dy}\right] + \left[k'(h^-(y))\frac{dh^+(y)}{dy} - k'(h^+(y))\frac{dh^+(y)}{dy}\right]\right) > 0 .$$

Equivalently,

$$c\left(k'(h^-(y))\left[\frac{dh^-(y)}{dy} - \frac{dh^+(y)}{dy}\right] + [k'(h^-(y)) - k'(h^+(y))]\frac{dh^+(y)}{dy}\right) > 0 .$$

We know from the shape of the cubic that $\frac{dh^{\pm}(y)}{dy} < 0$ on the left branches Provided that $c > 0$, $k' > 0$, and $k'' \geqq 0$, Condition (6) holds i $\frac{d}{dy}[h^+(y) - h^-(y)] < 0$, which can be checked by visual inspection of the I^- anc I^+ nullclines. Fig. 7 shows that (6) holds for the Ellias–Grossberg oscillator

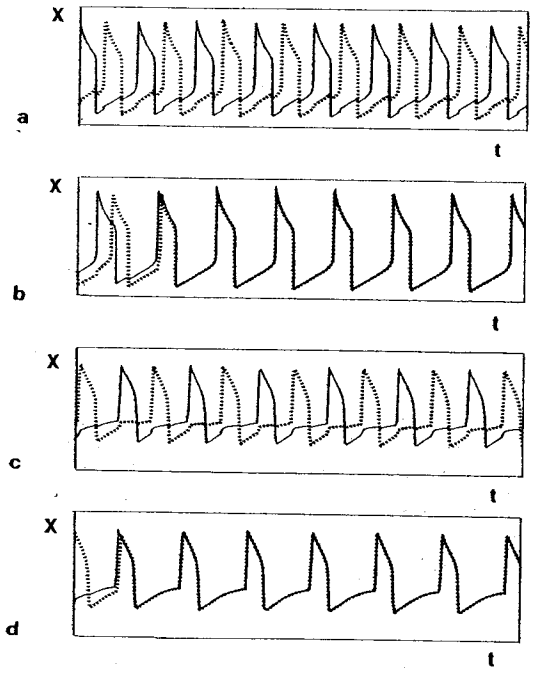

Fig. 8a–d. Bistability demonstration. **a, b** show the approach to the anti-phase and in-phase solutions, respectively, for a coupled pair of Morris–Lecar oscillators. **c, d** show anti-phase and in-phase solutions, respectively, for Ellias–Grossberg. In each bistability demonstration, only the initial conditions were varied between the in-phase and anti-phase trials. The domain of the in-phase solution was, in each case, larger than that of the anti-phase; the initial conditions for **b** and **d** start further from steady state than do those of **a** and **c**

Condition (6) also holds for the Morris–Lecar oscillator with the parameters stated above.

In Sect. 2, we gave hypotheses on a pair of coupled relaxation oscillators sufficient to insure the existence and stability of an anti-phase solution. In a previous paper [28], we gave other hypotheses on the same equations which are sufficient to insure that the in-phase solution is stable. The essential condition, which we called Condition C, was discussed in Remark 2.9. We argued in [28] why this condition should be expected to hold for a wide variety of relaxation oscillators, including equations that represent voltage-gated conduction models of nerve cells, such as Morris–Lecar [19] or network based models of nerve cells, such as Ellias–Grossberg [4] or Wilson–Cowan [34]. If Condition D and the stronger condition hypothesis iii) of Proposition 2.1 also hold, then the Morris–Lecar and Ellias–Grossberg equations exhibit bistability of in-phase and anti-phase solutions, as shown in Fig. 8. Circular arrays of these bistable oscillators with coupling between

nearest neighbors are capable of producing "fractured synchrony", a state i which there are domains of approximate synchrony with neighboring do mains having oscillators in approximate anti-phase. Fractured synchrony wa observed both for the Ellias–Grossberg and Morris–Lecar oscillators and thi array behavior is discussed in detail in [15].

Appendix

Proposition A.1. *Suppose that the hypotheses of Proposition* 2.1 *hold for th singular limit of* (2), (3). *Then there is a stable anti-phase solution to* (2), (3) *fo* $0 < \varepsilon \ll 1$.

Proof. The statement follows from the theorems of Mishchenko and Rozo [17] and Bonet [2], built on the work of Tikhonov [31]. The theorems ar technical, and we shall not give a full precise statement here. Roughly, th theorems hypothesize a singular periodic orbit whose slow portions lie o attracting slow manifolds, as we constructed in Sect. 2. They further requir that a certain "singular Poincaré map" have the singular orbit as an attractin fixed point. The conclusion of these theorems is that there is a nearby stabl anti-phase solution.

Rather than define the singular Poincaré map for general singularl perturbed equations, we shall explain what it is in the context of our equation and show why it has the required properties. The four-dimensional equation (2), (3) have two-dimensional attracting "slow manifolds" for the $\varepsilon = 0$ equa tions, corresponding to each oscillator lying on one of the outer branches o the $I = I^-$ or $I = I^+$ cubics. There are many pieces of the slow manifold corresponding to the choice of branch and cubic for each oscillator. The points at which one of the oscillators is at a knee lie on co-dimension one submanifolds (or curves) in these manifolds; it is at these curves that the singular solution can jump to another piece of the slow manifold. (One such "jump curve" consists of points with oscillator 1 at k_L^- and oscillator 2 on the left hand branch of $I = I^-$.) The singular solution constructed in Proposition 2.1 can be visualized in four-space as traveling among two pieces of the slow manifold in each half of its trajectory. For example, in the first hal of the trajectory, oscillator 1 starts on the right hand branch of the I^- cubic, while oscillator 2 is on the left hand branch of I^+, then both oscillators switch to the left hand branch of I^-; in the other half the oscillator indices are reversed.

The $\varepsilon = 0$ limit of (2), (3) induces a flow on these slow manifolds known as the "singular flow", with instantaneous jumps between the pieces. The jumps are governed by the "fast flow", in which $\hat{y}$ is constant and x, $\hat{x}$ satisfy $dx/d\xi = f(x, y, I(\hat{x}))$, $d\hat{x}/d\xi = f(\hat{x}, \hat{y}, I(x))$, where $\xi = \varepsilon t$ is fast time. From the singular flow and the fast jumps, a singular Poincaré map P_0 can be defined starting on a piece of a slow manifold near the singular solution: oscillator 1 starts at k_L^-, and oscillator 2 starts near the singular fixed point on the left

hand branch of the $I = I^-$ cubic. Let q be the position of oscillator 2 on the le hand branch of $I = I^-$ when oscillator 1 reaches k_L^-. The image under P_0 the point in 4-space for which oscillator 2 is at k_L^- and oscillator 1 is at q. No that P_0 is exactly the map $M(z)$ described before, but now considered a operating on submanifolds in 4-space. Proposition 2.1 shows that P_0 ha a stable fixed point corresponding to a singular periodic orbit in 4-space. No the theorems in [17] and [2] may be applied. □

Acknowledgments. We thank John Rinzel for his good questions and Larry Abbott fo helping to motivate work on interacting relaxation oscillators. We also thank the reviewer for their thoughtful and helpful comments.

References

1. Bélair, J., Holmes, P.: On linearly coupled relaxation oscillations. Quart. Appl. Math **42**, 193–219 (1984)
2. Bonet, C.: Singular perturbation of relaxed periodic orbits. J. Diff. Eq. **66**, 301–33 (1987)
3. Cronin, J.: Mathematical Aspects of Hodgkin–Huxley Neural Theory. Cambridge Cambridge University Press 1987
4. Ellias, S. A., Grossberg, S.: Pattern formation, contrast control, and oscillations in the short-term memory of shunting on-center, off-surround networks. Biol. Cybern. **20**, 69–98 (1975)
5. Ermentrout, G. B.: n:m phase-locking of weakly coupled oscillators. J. Math. Biol. **12**, 327–342 (1981)
6. Ermentrout, G. B., Kopell, N.: Oscillator death in systems of coupled neural oscillators. SIAM J. Appl. Math. **50**, 125–146 (1990)
7. Grasman, J.: Asymptotic Methods for Relaxation Oscillators and Applications. New York: Springer-Verlag 1987
8. Grossberg, S.: Some physiological and biochemical consequences of psychological postulates. Proc. Natl. Acad. Sci. (USA) **60**, 758–765 (1968)
9. Grossberg, S.: Contour enhancement, short-term memory, and constancies in reverberating neural networks. SIAM **52**, 217–257 (1973)
10. Hansel, D., Mato, G., Meunier, C.: Phase dynamics for weakly coupled Hodgkin–Huxley neurons. Europhys. Lett. **23**, 367–372 (1993)
11. Hodgkin, A. L., Huxley, A. F.: A quantitative description of membrane current and its application to conduction and excitation in nerve. J. Physiol. (London) **117**, 500–544 (1952)
12. Hoppensteadt, F. C.: An Introduction to the Mathematics of Neurons. Cambridge: Cambridge University Press 1986
13. Hoppensteadt, F. C., Keener, J. P.: Phase locking of biological clocks. J. Math. Biol. **15**, 339–349 (1982)
14. Jansen, M. J. W.: Synchronization of weakly coupled relaxation oscillators. Math. Centre, Amsterdam, Report TW 180 (1978)
15. Kopell, N., Somers, D.: Waves and synchrony in arrays of oscillators of relaxation and non-relaxation type (in preparation)
16. Krinskii, V. I., Pertsov, A. M., Reshetilov, A. N.: Investigation of one mechanism of origin of the ectopic focus of excitation in modified Hodgkin–Huxley equations. Biofizika **2**, 271–277 (1972)
17. Mishchenko, E. F., Rozov, N. Kh.: Differential equations with Small Parameters and Relaxation Oscillations. New York: Plenum Press 1980
18. Mirollo, R. E., Strogatz, S. H.: Synchronization of pulse-coupled biological oscillators. SIAM J. Appl. Math. **50**, 1645–1662 (1990)

19. Morris, C., Lecar, H.: Voltage oscillations in the barnacle giant muscle fiber. Biophys. J. **35**, 193–213 (1981)
20. Neu, J.: Coupled chemical oscillators. SIAM J. Appl. Math. **37**, 307–315 (1979)
21. Nordhaus, T.: Echo-cycles in coupled FitzHugh–Nagumo equations. Ph.D. Thesis, University of Utah 1988
22. Peskin, C. S.: Mathematical Aspects of Heart Physiology. New York: Courant Institute of Mathematical Sciences Publication 1975
23. Rand, R. H., Holmes, P. J.: Bifurcation of periodic motions in two weakly coupled van der Pol oscillators. Int. J. Nonlinear Mech. **15**, 387–399 (1980)
24. Rinzel, J.: On repetitive activity in nerve. FASEB Proc. **37**, 2793–2802 (1978)
25. Rinzel, J., Ermentrout, G. B.: Analysis of neural excitability and oscillations. In: C. Koch and I. Segev (eds.): Methods in Neuronal Modeling, pp. 135–169. Cambridge, MA: MIT Press 1989
26. Schöner, G., Kelso, J. A. S.: A synergetic theory of environmentally specified and learned patterns of movement coordination, II. Biol. Cybern. **58**, 81–89 (1988)
27. Sherman, A., Rinzel, J.: Rhythmogenic effects of weak electrotonic coupling in neuronal models. Proc. Natl. Acad. Sci. (USA) **89**, 2471–2474 (1992)
28. Somers, D., Kopell, N.: Rapid synchronization through fast threshold modulation. Biol. Cybern. **68**, 393–407 (1993)
29. Sperling, G., Sondhi, M. M.: Model for visual luminance discrimination and flicker detection. J. Optic. Soc. Am. **58**, 1133–1145 (1968)
30. Storti, D. W., Rand, R. H.: Dynamics of two strongly coupled relaxation oscillators. SIAM J. Appl. Math. **46**, 56–67 (1986)
31. Tikhonov, A.: On the dependence of solutions of differential equations on a small parameter. Math. Sbornik **22**, 193–204 (1948)
32. Torre, V.: Synchronization on nonlinear biochemical oscillators coupled by diffusion. Biol. Cybern. **17**, 137–144 (1975)
33. Wang, X.-J., Rinzel, J.: Alternating and synchronous rhythms in reciprocally inhibitory models neurons. Neur. Comp. **4**, 84–97 (1992)
34. Wilson, H. R., Cowan, J. D.: Excitatory and inhibitory interactions in localized populations of model neurons. Biophys. J. **12**, 1–24 (1972)